

DRAFT

Singlet fission tinkertoys based on N-heterocyclic carbenes: a study with the spin-flip simplified time-dependent density functional theory method

Gergana Kostadinova¹, Rumen Lyapchev¹, Joanna Stoycheva¹, Lyuben Borislavov¹, Alia Tadjer¹, Marc de Wergifosse,^{2,*} and Julia Romanova^{1,*}

¹*Sofia University, Faculty of Chemistry and Pharmacy, James Bourchier Blvd.1, Sofia 1164, Bulgaria*

²*Mulliken Centre for Theoretical Chemistry, Institut für Physikalische und Theoretische Chemie der Universität Bonn, Berings. 4, D-53115 Bonn, Germany*

Corresponding Authors

**jromanova@chem.uni-sofia.bg*

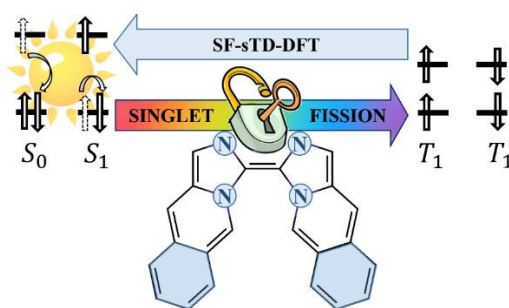
**mdewergifosse@gmail.com*

ABSTRACT

Singlet fission is a photophysical process in organic matter, in which one absorbed photon is converted in two triplet excitons. Discovered over 50 years ago, today singlet fission attracts scientific interest because it opens new horizons for the development of highly efficient organic-based solar cells beyond the Shockley–Queisser limit. However, a relatively small amount of singlet fission chromophores is available and, with respect to molecular design, little is known about the relationship between compounds' structure and singlet fission propensity. Here, we

report the molecular design of new singlet fission materials based on dimers of N-heterocyclic carbenes (NHC) and their 'locked' analogues. The study applies the recently introduced spin-flip simplified time-dependent density functional theory (SF-sTD-DFT) approach, which allows the modelling of sizeable molecules with diradical character like most of the successful singlet fission chromophores. To motivate the choice of method for the study NHC-based chromophores, the SF-sTD-DFT results are benchmarked against high level calculations using the equation-of-motion spin-flip coupled-cluster method with single and double substitutions. Armed with a reliable computational strategy, we have explored in detail the singlet fission propensity variation of the compounds due to the following structural factors: topology, type of substituents, *cis-trans* conformation, extension of the conjugation and modulation of the heterocyclic aromaticity, as well as the length of the latch in the 'locked' analogues. The results reveal new strategies for the design of singlet fission materials and contribute to the deeper understanding of the excited state tunability at the molecular level.

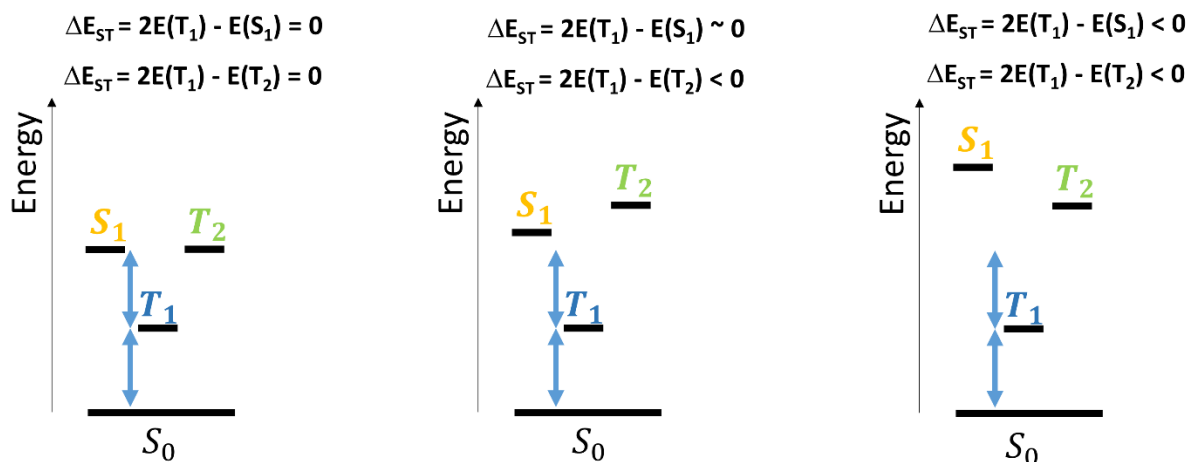
TOC GRAPHICS



KEYWORDS: sTDA, EOM-SF-CCSD, *cis-trans*, topology, Baird's rule, excited states, molecular orbitals, photovoltaics, solar cells, benchmarking

INTRODUCTION

Lately, the interest in organic photovoltaics has been renewed because of the renaissance of singlet fission – a photophysical process, which can boost the solar cells beyond the Shockley–Queisser limit.¹ In singlet fission, one absorbed photon is converted into two triplet excitons. Therefore, if utilized in solar cells, singlet fission may improve their efficiency by doubling the number of charge carriers.² The implementation of singlet fission should lead to the bright future for carbon-based photovoltaics but prior to this, we should face the challenge of finding out molecules able to undergo this process. Indeed, singlet fission chromophores for organic photovoltaics should satisfy a long list of requirements.³ First of all, twice the excitation energy to the first triplet excited state should be equal or less than the excitation energy to the first singlet excited state, $\Delta E_{ST} = 2E(T_1) - E(S_1) \lesssim 0$. Second, twice the excitation energy to the first triplet excited state must be less than the excitation energy to the second triplet excited state, $\Delta E_{TT} = 2E(T_1) - E(T_2) < 0$ (**Scheme 1**).



Scheme 1. Possible excited states arrangements in chromophores, which satisfy both feasibility conditions.

These two requirements are the primary singlet fission prerequisites, known as *feasibility conditions*. Furthermore, to harvest the maximum of the solar irradiation, these molecules must be characterized with a bright singlet excited state about 2 eV and consequently with $E(T_1) \sim 1$ eV. Finally, to be implemented in a real solar cell, these molecules should be stable under ambient conditions and photoexcitation. The latter is quite restrictive. It has been demonstrated that open-shell molecules with low to intermediate diradical character are among the best candidates that satisfy both feasibility conditions, but the open electron shell is usually related to high reactivity.⁴ In summary, compared to the voluminous group of conventional chromophores, only a small set of singlet fission chromophores is known and the structural variety within the set is relatively modest.³ Advancement in the field can be achieved by collecting more evidence on the relationship between chemical structure and singlet fission propensity, as

well as by exploring different strategies for molecular design. Moreover, the discovery of new structurally diverse chromophores will extend the margins of crystal engineering and will allow fine tunability of the singlet fission propensity at the supramolecular level.

So far, several fruitful strategies for creation of intermolecular singlet fission compounds have been reported and are briefly summarized here. Among them, extension of the π -conjugation has been elegantly illustrated in acenes, where singlet fission propensity grows progressively from naphthalene to pentacene.⁵ Another approach is the heteroatomic substitution (doping) with Si, B and N in polycyclic aromatic hydrocarbons.⁶⁻⁸ It has been demonstrated that in the doping strategy, molecular topology plays a crucial role for the singlet fission proclivity.⁹ The substituent effect has been explored in the case of thiophene dimers¹⁰, and very recently several papers appeared on the singlet fission potential of carbene scaffolds, namely cyclic (alkyl)(amino)carbenes (CAACs), known to stabilize radicals effectively.¹¹⁻¹³ The design strategy in these cases is based on the covalently bonded carbene units via π -conjugated molecular bridges of different length and type. The results showed that even the shortest bridges possess quite strong diradicaloid character. All of the above-mentioned examples reveal tactics for the creation of intermolecular singlet fission chromophores. The molecular design of such chromophores is a vital step but only an initial one in the material performance modelling, which is realized at the supramolecular level. The variation of the molecular bridge between dimers was demonstrated as a successful policy in the design of intramolecular singlet fission compounds, in which electronic states (S_0 and S_1) localized on the separate monomers interact to produce two independent spatially separated triplet excitons.¹⁴ Employing this methodology, covalently bound acenes¹⁵ and perylenes¹⁶ have been designed. Recently, the design methodologies have

gone beyond the dimer level and the construction of donor-acceptor copolymers has been shown as another successful way to create intramolecular singlet fission chromophores.¹⁷

Here, we present dimers of new N-heterocyclic carbenes (NHCs) (**Figure 1**) and demonstrate their singlet fission potential. The choice of compounds is inspired by the recently confirmed singlet fission proclivity of CAACs dimers^{12,13} and boron-doped polycyclic aromatic hydrocarbons⁷. The study on the latter revealed that polycyclic systems with boron, belonging to two adjacent rings, satisfy both feasibility conditions and are expected to minimize the thermal losses in singlet fission. As a result, the carbene dimers designed here consist of two NHCs, linked with a C=C bond, each monomer containing two nitrogens, one of which shared by adjacent cycles. Instead of playing with the type and π -conjugation length of the linker between the carbene units, we explored the effect of *cis*- or *trans*-conformation of the dimers on their singlet fission propensity. In addition, we have constructed NHC dimer analogues, 'locked' in *cis*-conformation by insertion of methylene latches between the two non-shared nitrogens, and investigated the effect of their length. And finally, all *cis*-, *trans*- and 'locked' NHC dimers allow functionalization with different type of substituents, which, depending on their electronic properties, position, π -conjugation length, and bulkiness, serve as additional tunability parameters of the excited states properties. Thus, combining and extending the two previously reported design strategies, we attained powerful molecular tinkertoys that allows the disclosure of new facets of the intimate relationship between structure and singlet fission propensity. The proposed NHC-derived chromophores are modelled based on synthetically realistic considerations and their experimental realization is achievable.

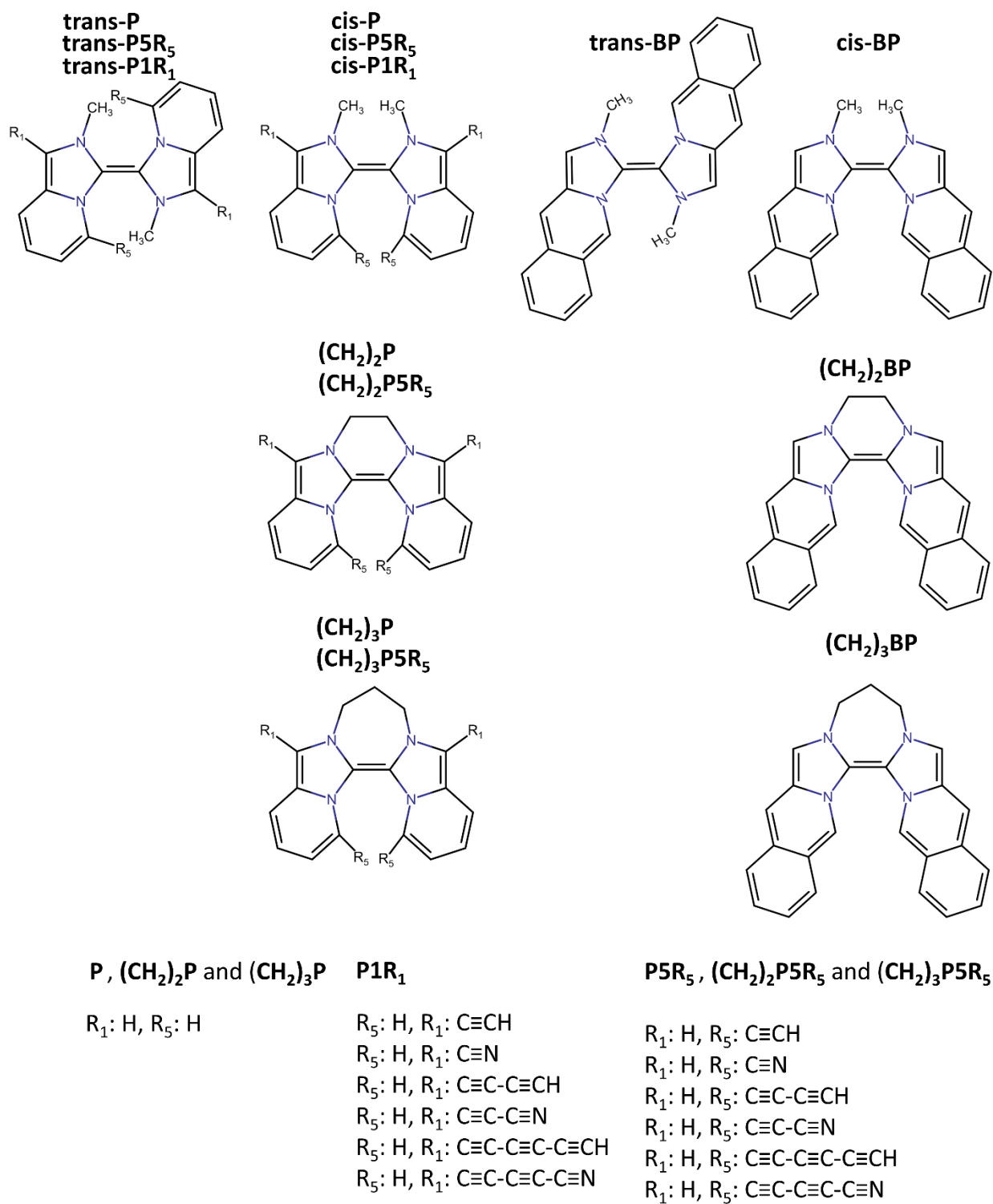


Figure 1. NHC dimers and their 'locked' analogues investigated in this work.

From synthetic point of view, activated positions for substitution in the heterocycles are **1** and **5**. In principle, both donor and acceptor types of substituents can be introduced at these sites. Taking into account that the monomer is non-aromatic (11 π -electrons), it can be expected that donor type of substituents will destabilize the ground state by increasing its antiaromatic character, while acceptor type of substituents will enhance its aromatic character. Therefore, all of the investigated compounds here contain acceptor type of substituents.

In addition to complementing molecular design strategies in the field, we propose a brand-new theoretical approach for studying singlet fission propensity of molecules using the recently developed spin-flip simplified time-dependent density functional theory method (SF-sTD-DFT).¹⁸⁻²⁰ The method is formulated for large chromophores with diradical character⁴ and features a high accuracy-to-computational cost ratio. It is a simplification of the popular spin-flip time-dependent density functional theory (SF-TD-DFT) method²¹⁻²⁴ that follows the spin-flip scheme²⁵ introduced by Krylov et al.²⁶⁻²⁹ to recover the missing static correlation in single reference methods, describing properly systems such as diradicals by including one doubly excited configuration. In the simplified version of the SF-TD-DFT method, considering the Tamm-Dancoff approximation and only collinear exchange-correlation (XC) functionals, the $(i_\alpha j_\alpha | a_\beta b_\beta)$ two-electron integrals between α occupied i and j and β unoccupied a and b molecular orbitals are approximated by short-range damped Coulomb interactions of transition density monopoles:

$$(i_\alpha j_\alpha | a_\beta b_\beta)' = \sum_A^N \sum_B^N q_{i_\alpha j_\alpha}^A q_{a_\beta b_\beta}^B \Gamma_{AB},$$

where the Mataga–Nishimoto–Ohno–Klopman short-range damped Coulomb operator is:

$$\Gamma_{AB}^{\alpha \rightarrow \beta} = \left(\frac{1}{(R_{AB})^{y_{\alpha \rightarrow \beta}} + (1.4 \times a_x \eta)^{-y_{\alpha \rightarrow \beta}}} \right)^{\frac{1}{y_{\alpha \rightarrow \beta}}}.$$

It depends on the amount of exact exchange a_x in the XC functional as well as on one parameter that reads:

$$y_{\alpha\rightarrow\beta} = a_x + 0.3.$$

This parameter was globally optimized for a benchmark set of nine diradicals.¹⁹ In addition, the space of single excitations is truncated according to a single energy threshold that represents the spectral range from 0 to E_{thresh} . These approximations drastically reduce the computational cost while retaining most of its accuracy.¹⁹ In the present study, the SF-STD-DFT method is particularly useful to screen large sets of compounds providing a better treatment of spin symmetry than the unrestricted DFT method. As it is the first time that this method is employed to describe NHC dimers, we benchmarked the SF-STD-DFT method against the high-level equation-of-motion spin-flip coupled-cluster method with single and double substitutions (EOM-sf-CCSD)^{25,27,30,31} to validate its use in this context. We also assessed whether the default value of $y_{\alpha\rightarrow\beta}$ is suitable for this class of compounds or if it should be adjusted.

This article is organized as follows: the *Computational protocol* contains benchmark results validating the choice of the SF-STD-DFT approach, as well as a description of the applied standard DFT methodology; the *Results and Discussion* section encompasses SF-STD-DFT results on the singlet fission propensity of the investigated compounds and their interpretation from molecular design standpoint; the *Conclusions* outline the key findings of the investigation, as well as perspectives on the photovoltaic implementation of the NHC dimers on the one hand, and on the applicability of the SF-STD-DFT approach to the study of singlet fission chromophores, on the other.

COMPUTATIONAL PROTOCOL

Validation of the utilization of the SF-STD-DFT approach for NHC singlet fission chromophores

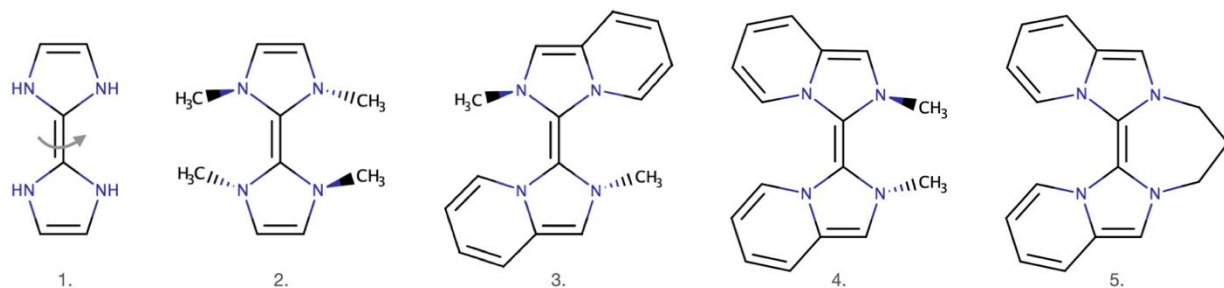


Figure 2: Model NHC structures, chosen to resemble the compounds in **Figure 1** – 1 and 2; 3 is **trans-P**, 4 is **cis-P** and 5 is **(CH₂)₂P**.

Figure 2 presents five N-heterocyclic carbene dimer model structures used to assess the suitability of the SF-STD-DFT method to compute the singlet-triplet energy gap, i.e., $E(T_1)$, for this class of compounds. We aim to find a suitable low-cost scheme to characterize such systems because some of their structures are too large to be treated with traditional methods. In that spirit, we compare the SF-STD-DFT/cc-pVDZ results to the EOM-sf-CCSD/aug-cc-pVTZ singlet-triplet energy gaps.

The whole range of the diradical character was explored for compound 1 by changing the dihedral angle between the two heterocycles. The geometries were optimized at the BH&HLYP/cc-pVDZ level of theory. Note that for compound 1, we performed a frozen scan from 0 to 180°. Reference calculations were performed with the EOM-SF-CCSD method. We froze core electrons, used the Cholesky decomposition with a threshold of 10^{-2} , and symmetries were not accounted for. SF-STD-DFT calculations were performed with the BH&HLYP exchange-correlation functional.

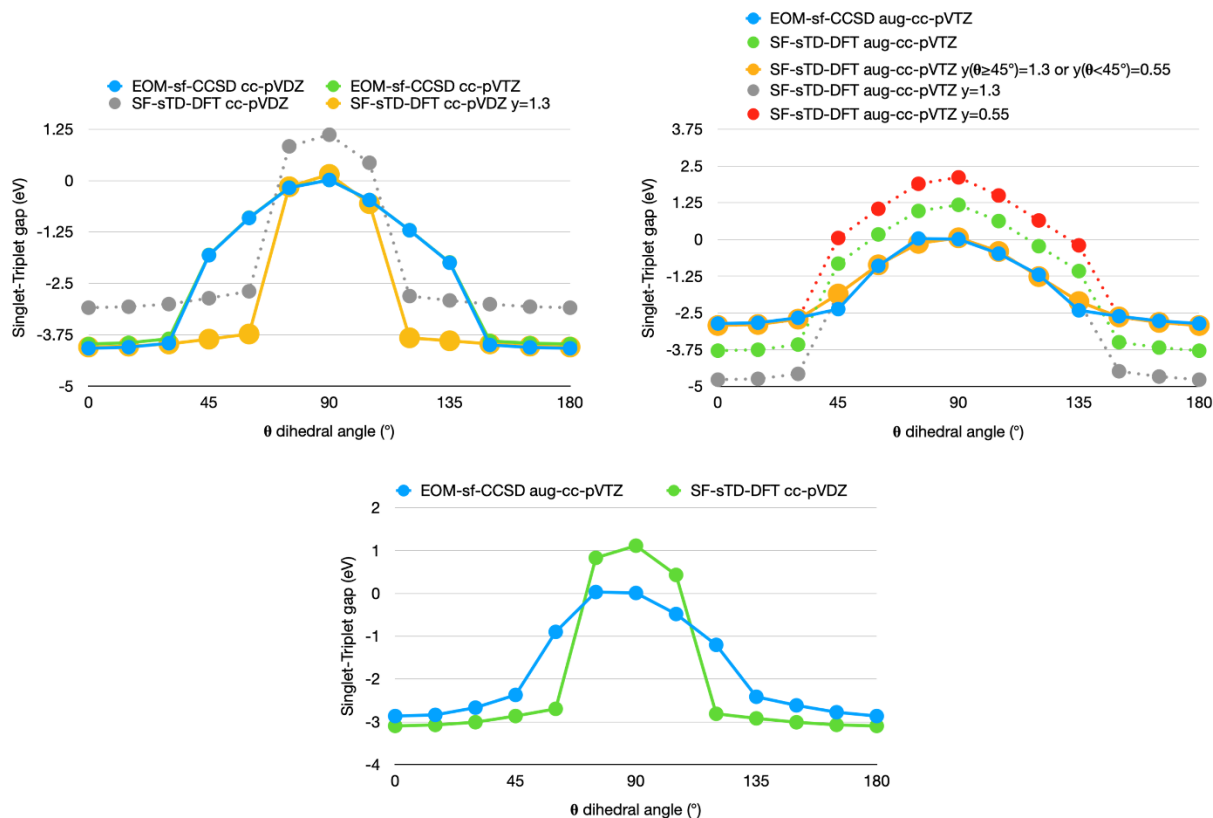


Figure 3: Singlet-Triplet gaps, $E(T_1)$, considering the whole range of dihedral angles for compound 1 obtained at both EOM-sf-CCSD and SF-sTD-DFT levels of theory with the cc-pVDZ, cc-pVTZ, and aug-cc-pVTZ basis sets. The sTD-DFT $y_{\alpha \rightarrow \beta}$ parameter was fine-tuned to reproduce better the reference calculations.

Figure 3 compares EOM-sf-CCSD reference singlet-triplet energy gaps to SF-sTD-DFT ones considering the whole range of dihedral angles for compound 1. Juxtaposition of the EOM-sf-CCSD results with the cc-pVDZ and cc-pVTZ basis sets reveals that they are almost identical. SF-sTD-DFT gaps are shifted to higher energies by about 25% with respect to reference calculations. Fine tuning the $y_{\alpha \rightarrow \beta}$ parameter from a value of 0.8 (BH&HLYP default value) to 1.3 allows a good reproduction of the reference calculations except for the angles of 45, 60, 120, and 135°. Adding

diffuse functions to the basis set decreases the energy difference between the values at 0 (or 180°) and 90° for EOM-sf-CCSD results. To reproduce best the EOM-sf-CCSD/aug-cc-pVTZ curve, the SF-sTD-DFT method was fine-tuned with $y_{\alpha\rightarrow\beta} = 0.55$ for angles smaller than 45° or larger than 135° and 1.3 for angles between 45° and 135°. Thus, EOM-sf-CCSD data are well-reproduced. Note that for the set of N-heterocyclic carbene dimers considered in this study, the deplanarization angle is always below 45° or above 135°. Below 45° or above 135°, the SF-sTD-DFT method reproduces well reference data with its default $y_{\alpha\rightarrow\beta}$ parameter, using the smaller cc-pVDZ basis set (see Figure 3, bottom panel).

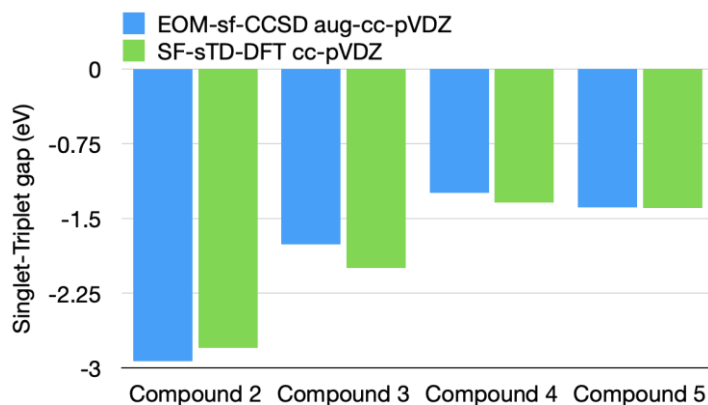


Figure 4: Singlet-triplet gaps, $E(T_1)$, for compounds 2-5 at the EOM-sf-CCSD/aug-cc-pVDZ and SF-sTD-DFT/cc-pVDZ levels of theory.

Figure 4 presents singlet-triplet energy gaps for compounds 2 to 5. Because the dihedral angle of compounds 2 to 5 is around 15, 0, 24, and 8° respectively, we used the SF-sTD-DFT method with the cc-pVDZ basis set to compare to EOM-sf-CCSD/aug-cc-pVDZ calculations. The agreement is striking, especially for such a level of approximations. It is worth noticing that for compound 3 the EOM-sf-CCSD calculation took 178 hours to run while the SF-sTD-DFT one took only a bit more than 4 minutes with the SCF step taking most of the time on the same 28 CPUs computer node.

Thus, the SF-sTD-DFT/cc-pVDZ level of theory with its default $y_{\alpha\rightarrow\beta}$ parameter is suitable to screen the set of NHC dimers considered in this study.

Theoretical estimation of the first and second feasibility conditions

All compounds presented in **Figure 1** were subject to ground state geometry optimization with the BH&HLYP functional and cc-pVDZ basis set, confirmed by vibrational frequencies analysis. The same basis set and functional were employed for both ground and excited state calculations. The vertical excitation energies $E(S_1)$ and $E(T_1)$, as well as the first feasibility condition ΔE_{ST} , were estimated with the SF-sTD-DFT method. In the SF-sTD-DFT calculations, the triplet reference is obtained from triplet single point calculations with the BH&HLYP/cc-pVDZ method on top of the optimized singlet ground state geometries. The transition dipole moments between SF states obtained at the SF-sTD-DFT level of theory are multiplied by a factor of $\sqrt{2}$ to correct for missing excitation in the α space.¹⁹ The same high-spin triplet reference is used for the estimation of the vertical excitation energies $T_1\rightarrow T_2$ with the unrestricted sTDA approach.¹⁹ Because open-shell solutions for high-spin triplet are usually well-behaved in term of spin contamination, the SF procedure was not involved in this step. The $T_1\rightarrow T_2$ energy difference is then added to $E(T_1)$ to approximate the vertical excitation energy $S_0\rightarrow T_2$, i.e. $E(T_2)$. Thereafter, the second feasibility condition energies ΔE_{TT} were also estimated.

The simulations were performed with the Gaussian 09³² (DFT) and Q-CHEM 5.1³³(EOM-SF-CCSD) program packages, as well as with the open-access stda code (SF-sTD-DFT/sTDA)³⁴. The molecular orbitals were visualized using GaussView 06 and isosurface value of 0.02.

RESULTS AND DISCUSSION

Results on the effect of *cis*- and *trans*- conformations of NHC dimers on the vertical excitation energies and feasibility conditions (ΔE_{ST} and ΔE_{TT}) are summarized in **Table 1**. The values for ΔE_{ST} in all *cis*-conformers are smaller, compared to the *trans*-ones, which reveals high potential of the *cis*-conformation for singlet fission. The isomerization from *cis*- to *trans*- destabilizes the key excited states (S_1 , T_1 and T_2). Such a raise in vertical excitation energies is substantial and amounts to at least 0.6 eV for S_1 , 0.5 eV for T_1 and 0.3 eV for T_2 . The conformational dependent singlet fission propensity can be explained by the larger steric hindrance in the *cis*-forms with respect to the *trans*-ones. Evidence, supporting this suggestion, can be extracted from the values of the dihedral angle between the carbene units, which show that all *cis*-forms exhibit deviation from planarity (**Table 1**). The results for the ground state *cis*-structures reveal that the introduction of substituent at position **1** leads to smaller deplanarization (23°), compared to functionalization at position **5** (33°). In all *cis*-conformers the inter-ring bond length is about 1.36 Å, while in the *trans*-forms it is about 1.35 Å (**Table 1**). This suggests that the deplanarization of the dimers is also accompanied with a slight weakening of the conjugation between the carbene units.

The position to which substituents are attached is also of paramount importance for the excited states properties and singlet fission propensity of the dimers. This can be demonstrated with the $-\text{C}\equiv\text{N}$ group as a substituent, which is a small and conformationally rigid strong acceptor. For example, ΔE_{ST} for the dimers with $-\text{C}\equiv\text{N}$ substituents decreases with $\sim 0.4\text{-}0.5$ eV when switching position from **1** to **5**. This is valid for both *cis*- and *trans*-conformers; hence, this effect cannot be explained solely by the electronic properties of the substituents' and dimers' conformation. To

gain more insight into this trend, we inspected carefully the singly occupied molecular orbitals (SOMOs) for the triplet reference of compounds **cis-P1-C≡CH** and **cis-P5-C≡CH** (Figure 5). They correspond mostly to the HOMO and LUMO in the ground SF singlet state because both structures present negligible diradical characters, evidenced by their relatively high $E(T_1)$. The SOMOs examination reveals that when attached to position **5**, the **-C≡N** substituents participate in one of the lower in energy SOMO and have negligible coefficients in the other one, while opposite behaviour is observed for position **1**. In both isomers, the lower in energy SOMOs span in an identical manner over the main skeleton of the dimer and the coefficient of the substituent in a given MO is proportional to the coefficient of the carbons to which the substituent is bonded. Since the lower in energy SOMOs are characterized with negligible coefficient at position **5**, the different behaviour of the substituent in this isomer can be explained with a zero overlap with the dimers' main skeleton. Therefore, it might be speculated that the functionalization at position **5** favours the charge transfer from the carbene units to the **-C≡N** substituents in the excited state. This in turn decreases the excitation energies and the ΔE_{ST} values for **P5-C≡N** with respect to **P1-C≡N** isomers. The effect of the substituent's position on the excited state properties can be explained by the resonance structures and Baird's rule³⁵ (Figure 6). Functionalization with **-C≡N** groups at position **5** leads to charge transfer from the N-CH₃ nitrogens to the substituents, while attaching the same groups at position **1** causes charge transfer from the intercylic nitrogens to the substituents. The N-CH₃ nitrogens are expected to be stronger electron donors in the dimers. Moreover, in line with the Baird's rule, the difference in the excited state conjugation pattern can explain the variation in the excited state energy as a function of the substituent position. The Baird's rule states that the energy of the T_1 increases when $4n+2$ cycles are formed in the excited

state, i.e. $4n+2$ cycles in the excited state are deemed antiaromatic. The Baird's rule was recently applied as a strategy for the modelling of singlet fission materials and shows correlation with both S_1 and T_1 excited state energies.³⁶ When $-C\equiv N$ groups are attached to positions **1** of the dimer, both heterocycles become antiaromatic ($4n+2$) in the excited state. On the other hand, the functionalization at positions **5** causes excited state antiaromatization only of the five membered rings. Therefore, the S_1 and T_1 excited state energies are lower in the isomers functionalized at positions **5** than in the case of conformers with substituents at positions **1**. The smallest ΔE_{ST} (~ 0.27 eV) in the *cis-trans* series with substituents is predicted for *cis-P5-C \equiv C-C \equiv C-C \equiv N*, which suggests the possibility for endothermic singlet fission in this compound.

Surprisingly, among all key excitation energies, the tunability in $E(T_2)$ as a function of the substituents is most pronounced. For example, going from *cis-* to *trans-*, the $E(T_2)$ excitation energy decreases from 2.07 eV for **P5-C \equiv CH** to 0.33 eV for **P**. However, despite the high tunability in $E(T_2)$, in all *cis-trans* cases with substituents, the second feasibility condition is also positive, which indicates high probability for triplet-triplet annihilation in such compounds and therefore, inefficient singlet fission.

Beside the substituent effect, the conjugation length of the carbene skeleton is another factor that can affect the excited state properties of the dimers. The addition of benzene rings to the heterocycles has a dramatic effect on the singlet fission propensity of the compounds even when no substituents are attached to positions **5** and **1**. Comparing molecules **P** and **BP**, it is visible that the polycyclic system extension decreases ΔE_{ST} from 1.84 to 1.07 eV for the *trans*-forms and from 1.17 to 0.18 eV for the *cis*-ones. The structural modification affects both S_1 and T_1 and lowers

their energy by 0.8-1.0 eV both in the *cis*- and *trans*-forms. Consequently, the *cis*-form of **BP** is predicted as slightly exergonic singlet fission material. Moreover, BP is the only compound in the *cis-trans* series for which the second feasibility condition is negative suggesting again its high singlet fission propensity.

Before finalizing the *cis-trans* comparison, it is worth noticing that at the BH&HLYP level of theory, the steric hindrance in the *cis*- forms does not necessarily have a negative impact on their thermodynamic stability (**Table S1** and **Discussion S1, SI**).

Table 1. Singlet fission feasibility conditions ΔE_{ST} [eV] and ΔE_{TT} [eV]; vertical excitation energies to the first singlet $E(S_1)$ [eV], first triplet $E(T_1)$ [eV] and second triplet $E(T_2)$ [eV] excited states; oscillator strength for the $S_0 \rightarrow S_1$ transition. Inter-ring bond length $R[\text{\AA}]$ and dihedral angle Θ [$^\circ$] between the carbene units from the BH&HLYP optimized geometries.

Compound	Form	$E(S_1)$	f	$E(T_1)$	$E(T_2)$	ΔE_{ST}	ΔE_{TT}	Θ	R
P	<i>trans</i>	2.13	0.0110	1.99	2.02	1.84	1.95	180	1.346
P	<i>cis</i>	1.51	0.0050	1.34	1.69	1.17	0.99	22	1.353
P5-C \equiv CH	<i>trans</i>	1.86	0.0098	1.74	3.21	1.63	0.27	180	1.352
P5-C \equiv CH	<i>cis</i>	1.17	0.0049	0.97	1.14	0.77	0.81	34	1.359
P5-C \equiv N	<i>trans</i>	1.78	0.0086	1.63	3.18	1.49	0.08	180	1.350
P5-C \equiv N	<i>cis</i>	1.09	0.0023	0.84	1.06	0.58	0.62	33	1.357
P5-C \equiv C-C \equiv CH	<i>trans</i>	1.65	0.0126	1.53	2.86	1.41	0.21	180	1.351
P5-C \equiv C-C \equiv CH	<i>cis</i>	0.97	0.0061	0.76	0.91	0.56	0.61	33	1.357
P5-C \equiv C-C \equiv N	<i>trans</i>	1.57	0.0116	1.44	2.79	1.31	0.10	180	1.350
P5-C \equiv C-C \equiv N	<i>cis</i>	0.86	0.0039	0.61	0.78	0.37	0.45	33	1.356
P5-C \equiv C-C \equiv C-C \equiv CH	<i>trans</i>	1.52	0.0171	1.41	2.38	1.29	0.44	180	1.351
P5-C \equiv C-C \equiv C-C \equiv CH	<i>cis</i>	0.83	0.0075	0.62	0.74	0.42	0.51	33	1.357
P5-C \equiv C-C \equiv C-C \equiv N	<i>trans</i>	1.43	0.0177	1.31	2.15	1.19	0.47	180	1.350
P5-C \equiv C-C \equiv C-C \equiv N	<i>cis</i>	0.71	0.0066	0.49	0.61	0.27	0.37	32	1.356
P1-C \equiv CH	<i>trans</i>	2.09	0.0151	1.95	3.32	1.81	0.58	180	1.345
P1-C \equiv CH	<i>cis</i>	1.40	0.0069	1.24	1.56	1.07	0.92	23	1.355

P1-C≡N	<i>trans</i>	2.21	0.0134	2.05	2.06	1.89	2.05	180	1.343
P1-C≡N	<i>cis</i>	1.45	0.0076	1.27	1.65	1.09	0.90	23	1.354
P1-C≡C-C≡CH	<i>trans</i>	2.04	0.0218	1.91	3.08	1.78	0.75	180	1.345
P1-C≡C-C≡CH	<i>cis</i>	1.33	0.0095	1.18	1.46	1.02	0.89	24	1.356
P1-C≡C-C≡N	<i>trans</i>	2.10	0.0180	1.97	3.13	1.83	0.80	180	1.344
P1-C≡C-C≡N	<i>cis</i>	1.34	0.0093	1.17	1.49	1.01	0.86	24	1.356
P1-C≡C-C≡C-C≡CH	<i>trans</i>	2.00	0.0318	1.88	2.85	1.76	0.90	180	1.344
P1-C≡C-C≡C-C≡CH	<i>cis</i>	1.28	0.0131	1.13	1.39	0.98	0.87	24	1.356
P1-C≡C-C≡C-C≡N	<i>trans</i>	2.02	0.0296	1.90	2.82	1.79	0.99	180	1.344
P1-C≡C-C≡C-C≡N	<i>cis</i>	1.27	0.0132	1.11	1.38	0.96	0.84	24	1.357
BP	<i>trans</i>	1.33	0.0210	1.20	2.43	1.07	-0.03	180	1.349
BP	<i>cis</i>	0.60	0.0061	0.39	0.82	0.18	-0.04	24	1.364

Encouraged by the revealed structure-properties relationships in the *cis-trans* series, we have constructed synthetically reasonable ‘locked’ *cis*-analogues with substituents at position 5 and larger polycyclic system (**Figure 1**). The locking of the NHC dimers is ensured by the insertion of two or three CH₂ groups between the non-shared nitrogen atoms. The advantages of the ‘locked’ dimers are as follows: 1) fixing the structure with CH₂-groups will reduce the possibility for free rotation around the inter-ring bond and thus will minimize the energy losses in singlet fission, 2) the molecular “latch” prevents but does not prohibit deplanarization and this can be used as an additional factor for fine tuning of the excited state properties, and 3) keeping optimal deplanarization should facilitate supramolecular ordering and crystal packing.

Results on the structure, vertical excitation energies, and feasibility conditions (ΔE_{ST} and ΔE_{TT}) for the ‘locked’ NHC dimers are summarized in **Table 2**. As expected, for a given positional analogue from the *cis-trans* series, locking of the *cis*-forms reduces the ΔE_{ST} energy differences and, therefore, the conformational strategy for design works generally well. Smaller degree of deplanarization is observed when the molecular latch is -CH₂-CH₂- (17°) than when it is -CH₂-CH₂-

CH₂- (34°) and in all cases the inter-ring bond is about 1.36 Å. As a result of the stronger conformation fixing, the substituent effect on the singlet fission propensity of the compounds is not well pronounced for the -CH₂-CH₂- 'locked' dimers. As a function of the substituents, the ΔE_{ST} energy differences vary between 0.3 - 1.0 eV for the -CH₂-CH₂-CH₂- 'locked' dimers and within 0.5-1.3 eV in the case of the -CH₂-CH₂- latch. This trend reveals that a substantial portion of the substituent effect in the NHC dimers originates from its bulkiness and the possibility for deplanarization. Moreover, it is interesting to note that after comparing dimers that differ only in the molecular latch, it turns out that in all -CH₂-CH₂- cases the S₁ and T₁ excitation energies are, respectively, lower and higher than those of the -CH₂-CH₂-CH₂- 'locked' dimers. Lower T₂ excitation energies are observed for the substituent-containing dimers with -CH₂-CH₂-CH₂- latch, while opposite behaviour is seen for the 'locked' cases without functional groups. Therefore, it is not surprising that ΔE_{ST} values for the -CH₂-CH₂- 'locked' dimers remain relatively high and that ΔE_{TT} values for these compounds are negative (except for the non-substituted ones). On the other hand, three -CH₂-CH₂-CH₂- 'locked' dimers are predicted as slightly exergonic singlet fission materials: **(CH₂)₃P5-C≡C-C≡N** (ΔE_{ST}=0.32 eV), **(CH₂)₃P5-C≡C-C≡C-C≡N** (ΔE_{ST}=0.28 eV) and **(CH₂)₃P5-C≡C-C≡C-C≡CH** (ΔE_{ST}=0.37 eV). Among all -CH₂-CH₂-CH₂- 'locked' dimers, these three compounds contain substituents with the longest conjugation path. And since the bulkiness of the non-hydrogen substituents in the -CH₂-CH₂-CH₂- series is similar (they vary only in length), the positive effect on ΔE_{ST} is mainly due to the extension of the π-electron system by addition of 1 or 2 triple bonds per functional group. Moreover, there is a simultaneous decrease in both S₁ and T₁ excitation energies with an increase in the conjugation length of the substituents, estimated at approximately 0.05 eV per triple bond. Unfortunately, compounds **(CH₂)₃P5-C≡C-C≡N**, **(CH₂)₃P5-**

C≡C-C≡C-C≡N and **(CH₂)₃P5-C≡C-C≡C-C≡CH** do not satisfy the second feasibility condition and therefore they cannot be regarded as efficient singlet fission materials.

Table 2. Singlet fission feasibility conditions ΔE_{ST} [eV] and ΔE_{TT} [eV]; vertical excitation energies to the first singlet $E(S_1)$ [eV], first triplet $E(T_1)$ [eV] and second triplet $E(T_2)$ [eV] excited states; oscillator strength for the $S_0 \rightarrow S_1$ transition. Inter-ring bond length R [Å] and dihedral angle Θ [°] between the carbene units from the BH&HLYP optimized geometries.

Compound	$E(S_1)$	f	$E(T_1)$	$E(T_2)$	ΔE_{ST}	ΔE_{TT}	Θ	R
(CH₂)₂P	1.62	0.0031	1.46	1.48	1.30	1.44	14	1.348
(CH₂)₂P5-C≡CH	1.38	0.0037	1.24	2.80	1.10	-0.32	17	1.355
(CH₂)₂P5-C≡N	1.26	0.0020	1.09	2.62	0.92	-0.45	17	1.355
(CH₂)₂P5-C≡C-C≡CH	1.13	0.0048	0.98	2.34	0.84	-0.38	17	1.355
(CH₂)₂P5-C≡C-C≡N	0.96	0.0033	0.80	2.11	0.63	-0.51	17	1.354
(CH₂)₂P5-C≡C-C≡C-C≡CH	0.95	0.0063	0.80	1.70	0.66	-0.09	17	1.354
(CH₂)₂P5-C≡C-C≡C-C≡N	0.78	0.0056	0.63	1.41	0.49	-0.14	17	1.354
(CH₂)₂BP	0.77	0.0050	0.33	1.03	-0.11	-0.37	14	1.356
(CH₂)₃P	1.79	0.0023	1.39	2.07	1.00	0.71	25	1.353
(CH₂)₃P5-C≡CH	1.46	0.0022	1.03	1.54	0.60	0.52	34	1.359
(CH₂)₃P5-C≡N	1.37	0.0010	0.91	1.40	0.45	0.41	34	1.357
(CH₂)₃P5-C≡C-C≡CH	1.26	0.003	0.85	1.20	0.45	0.50	34	1.357
(CH₂)₃P5-C≡C-C≡N	1.13	0.0022	0.72	0.98	0.32	0.47	34	1.357
(CH₂)₃P5-C≡C-C≡C-C≡CH	1.11	0.0052	0.74	0.96	0.37	0.52	34	1.357
(CH₂)₃P5-C≡C-C≡C-C≡N	0.97	0.0067	0.63	0.75	0.28	0.51	34	1.357
(CH₂)₃BP	0.87	0.01	0.44	1.22	0.00	-0.35	27	1.361

Another approach for increasing the conjugation path in the ‘locked’ NHC dimers is the attachment of condensed benzene rings to the heterocycles. Applying this strategy, two promising singlet fission materials are designed: **(CH₂)₂BP** with $\Delta E_{ST} = -0.11$ eV and **(CH₂)₃BP** with $\Delta E_{ST} = 0.00$ eV. As in the case of the *cis-trans* series, the expansion of the polyaromatic system has stronger effect on the singlet fission propensity than the extension of the conjugation in the

exocyclic substituents. When compared with the parent compounds $(\text{CH}_2)_2\text{P}$ and $(\text{CH}_2)_3\text{P}$, the decrease in ΔE_{ST} from benzene ring addition is about 1.41 eV and 1.00 eV, respectively. Moreover, both $(\text{CH}_2)_2\text{BP}$ and $(\text{CH}_2)_3\text{BP}$ satisfy the second feasibility condition and are, therefore, among the best singlet fission candidates reported here. As it can be expected, the condensation of benzene cycles lowers all key excitation energies – to the S_1 , T_1 and T_2 states. However, the stabilization effect is slightly more pronounced in T_1 (1.13 eV) than in S_1 (0.85 eV) and T_2 (0.45 eV) for the $-\text{CH}_2-\text{CH}_2-$ latched dimers and similar for all excited states in the $-\text{CH}_2-\text{CH}_2-\text{CH}_2-$ containing compounds (0.9-1.0 eV).

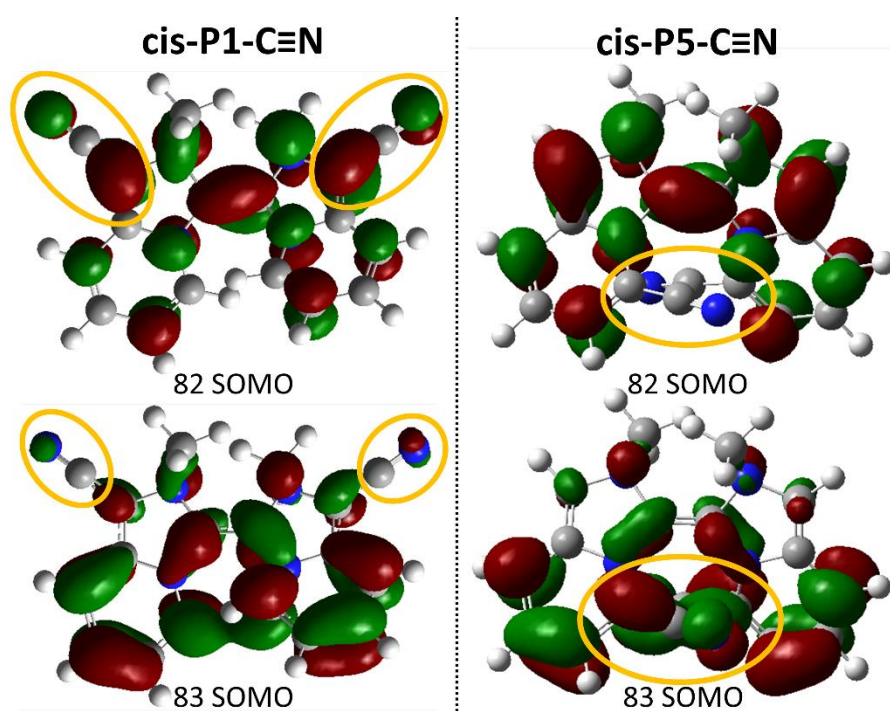


Figure 5. SOMOs in the triplet reference wavefunction as a function of the substituent position obtained at the BH&HLYP/cc-pVDZ level of theory. The isosurface value is 0.03.

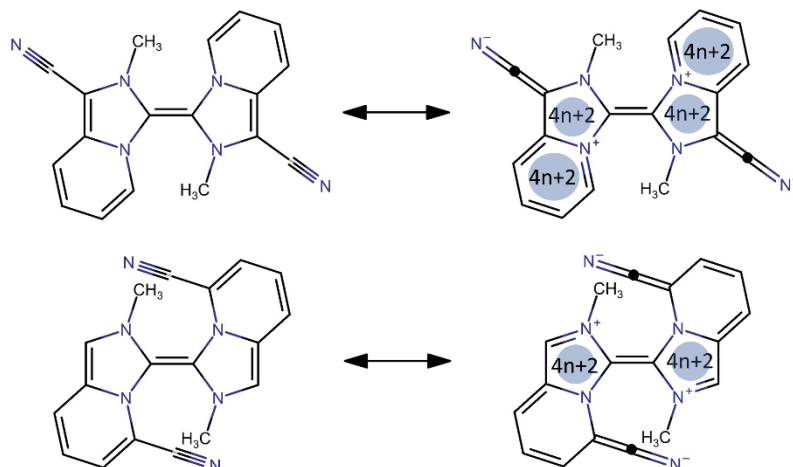


Figure 6. Resonance structure in the ground (left) and excited (right) state as a function of the substituent position.

Finally, from the perspective of photovoltaics application, we should discuss the absorption cross sections for the best singlet fission candidates: *cis*-BP, (CH₂)₂BP and (CH₂)₃BP. The SF-sTD-DFT results indicate that all these compounds are characterized with an almost 'dark' S₁ excited state lying in the NIR region (Table 2).

Table 3. SF-sTD-DFT/cc-pVDZ results for most intensive NIR and UV-vis excitations in the best singlet fission candidates: E(S_n) [eV] – excitation energy and f – oscillator strength.

Compound	E(S _n) ^{NIR}	f ^{NIR}	E(S _n) ^{UV/UV-vis}	f ^{UV/UV-vis}
<i>cis</i> -BP	1.16	0.1418	2.97	0.0472
(CH ₂) ₂ BP	1.21	0.0811	2.95	0.1266
(CH ₂) ₃ BP	1.38	0.0852	3.12	0.1234

However, they absorb in the NIR, as well as in the UV-vis and near-UV region (Table 3). For all three compounds the brightest NIR excited state is S₄ and the UV/UV-vis one is S₈. The results indicate that the proposed compounds are not conventional singlet fission materials with bright

S_1 states lying in the UV-vis region. On the other hand, it was demonstrated that a successful strategy for achieving high efficiencies in organic solar cells is the incorporation of materials absorbing in the NIR region, which contains about 40% of the solar power.³⁷ Therefore, it can be speculated that the presence of a singlet fission material absorbing at both NIR and UV-vis regions might ensure capturing of a broad range of wavelengths from the solar spectrum and would have a positive impact on the solar cell efficiency. Such positive impact might balance the thermal losses from the $S_n \rightarrow S_1$ decay, but since the photophysics of singlet fission materials is rich, only the real experiment can prove or deny the usefulness of such compounds.

Lastly, from an application perspective, note that for many of the investigated compounds the vertical excitation energies to S_1 and T_1 are very close. This finding is independent of the type of substituent, its position or conformation. Therefore, some of the designed NHC dimers have the potential to become attractive UV-vis and near-infrared thermally activated delayed fluorescent materials.³⁸ This is the case for e.g., the **trans-P1-C \equiv C-C \equiv CH**, **trans-BP**, **trans-P1-C \equiv C-C \equiv C-C \equiv N**, and **trans-P1-C \equiv C-C \equiv C-C \equiv CH**, which are also characterized with bright first excited states.

CONCLUSIONS

We have designed new NHC dimers and their 'locked' analogues, which have the potential to serve as singlet fission chromophores in solar cells. The compounds represent molecular tinkertoys, which allowed us to explore a variety of structure-properties relationships from singlet fission perspectives, such as the independent or simultaneous influence of the following factors: topology, type of substituents, *cis-trans* conformation, extension of the conjugation and modulation in the heterocyclic aromaticity, as well as the length of the latch in the 'locked'

analogues. The compounds are relatively large in size for conventional multiconfigurational approaches. Therefore, to reveal their singlet fission potential, we have applied the computationally less-demanding spin-flip sTD-DFT method, especially developed for large diradicals. For this purpose, the spin-flip sTD-DFT method was benchmarked with respect to the EOM-sf-CCSD level of theory for a set of five NHC model compounds. The method shows excellent performance in estimating the problematic $E(T_1)$ energy and good cost-accuracy ratio. The results demonstrate that strong tunability in the singlet fission propensity of these compounds can be achieved by *cis-trans* conformational changes, extension of the conjugation length through annulation and playing with substituent topology. The substituent topology effect is explained in terms of Baird's aromaticity. On the other hand, we demonstrate that fine tunability can be reached by modulation of conjugation length within the substituents and extension of the latch in the 'locked' analogues. As a result of the detailed analysis, three promising singlet fission candidates are highlighted and all of them possess *cis*-type of conformation: ***cis*-BP** and the 'locked' **(CH₂)₂BP** and **(CH₂)₃BP**. The three compounds are characterized with 'dark' first excited states and absorb intensively in the NIR, as well as in the UV-vis/end of UV regions. Among the candidates not suitable for singlet fission they are NHC carbene dimers, which seem potential UV-vis and near-infrared thermally activated delayed fluorescent materials.

ACKNOWLEDGEMENTS

The authors acknowledge the financial support of the Bulgarian National Science Fund, contract КП-06-H39/2 from 09.12.2019, the National Research Program E+, DMC 577/17.08.2018, grant agreement D01-214/28.11.2018, MdeW thanks the DFG for its support in the framework of the

project "Theoretical studies of nonlinear optical properties of fluorescent proteins by novel low-cost quantum chemistry methods" (Nr. 450959503).

References:

1. W. Shockley and H.J. Queisser, Detailed balance limit of efficiency of p-n junction solar cells. *J. Appl. Phys.* 1961, **32**, 510-519.
2. M.C. Hanna and A.J. Nozik, Solar conversion efficiency of photovoltaic and photoelectrolysis cells with carrier multiplication absorbers. *J. Appl. Phys.* 2006, **100**, 074510.
3. M.B. Smith and J. Michl, Singlet fission. *Chem. Rev.* 2010, **110**, 6891-6936.
4. T. Minami, and M. Nakano, Diradical character view of singlet fission. *J. Phys. Chem. Lett.* 2011, **3**, 145-150.
5. M.B. Smith and J. Michl, Recent advances in singlet fission. *Annu. Rev. Phys. Chem.* 2013, **64**, 361-386.
6. T. Zeng, N. Ananth, and R. Hoffmann, Seeking Small Molecules for Singlet Fission: A Heteroatom Substitution Strategy. *J. Am. Chem. Soc.* 2014, **136**, 12638–12647.
7. J. Stoycheva, A. Tadjer, M. Garavelli, M. Spassova, A. Nenov and J. Romanova, Boron-doped polycyclic aromatic hydrocarbons: a molecular set revealing the interplay between topology and singlet fission propensity. *J. Phys. Chem. Lett.* 2020, **11**, 1390-1396.
8. T. Zeng, S.K. Mellerup, D. Yang, X. Wang, S. Wang and K. Stamplecoskie, Identifying (BN)₂-pyrenes as a new class of singlet fission chromophores: significance of azaborine substitution. *J. Phys. Chem. Lett.* 2018, **9**, 2919–2927.
9. S. Ito and M. Nakano, Theoretical molecular design of heteroacenes for singlet fission: tuning the diradical character by modifying π -conjugation length and aromaticity. *J. Phys. Chem. C* 2015, **119**, 148-157.
10. L. Shen, X. Wang, H. Liu and X. Li, Tuning the singlet fission relevant energetic levels of quinoidal bithiophene compounds by means of backbone modifications and functional group introduction. *Phys. Chem. Chem. Phys.* 2018, **20**, 5795.
11. J. Messelberger, A. Grünwald, P. Pinter, M.M. Hansmann and D. Munz, Carbene derived diradicaloids – building blocks for singlet fission? *Chem. Sci.* 2018, **9**, 6107-6117.
12. A. Japahuge, S. Lee, C.H. Choi and T. Zeng, Design of singlet fission chromophores with cyclic (alkyl)(amino)carbene building blocks. *J. Chem. Phys.* 2019, **150**, 234306.
13. T. Ullrich, P. Pinter, J. Messelberger, P. Haines, R. Kaur, M.M. Hansmann, D. Munz and D.M. Guldi, Singlet fission in carbene-derived diradicaloids. *Angew. Chem.* 2020, **59**, 7906-7914.
14. S. Ito, T. Nagami and M. Nakano, Design principles of electronic couplings for intramolecular singlet fission in covalently-linked systems. *J. Phys. Chem. A* 2016, **120**, 6236-6241.

15. X. Feng, D. Casanova and A.I. Krylov, Intra- and intermolecular singlet fission in covalently linked dimers *J. Phys. Chem. C* 2016, **120**, 19070-19077.
16. N.V. Korovina, N.F. Pompetti and J.C. Johnson, Lessons from intramolecular singlet fission with covalently bound chromophores. *J. Chem. Phys.* 2020, **152**, 040904.
17. J.T. Blaskovits, M. Fumanal, S. Vela and C. Corminboeuf, Designing singlet fission candidates from donor-acceptor copolymers. *Chem. Mater.* 2020, **32**, 6515-6524.
18. M. de Wergifosse, J. Seibert, B. Champagne and S. Grimme, Are fully conjugated expanded indenofluorenes analogues and diindeno[n]thiophene derivatives diradicals? A simplified (spin-flip) time-dependent density functional theory [(SF)sTD-DFT] study, *J. Phys. Chem. A* 2019, **123**, 9828-9839.
19. M. de Wergifosse, C. Bannwarth and S. Grimme, A simplified spin-flip time-dependent density functional theory approach for the electronic excitation spectra of very large diradicals. *J. Phys. Chem. A* 2019, **123**, 5815-5825.
20. M. de Wergifosse and S. Grimme, Perspective on simplified quantum chemistry methods for excited states and response properties. *J. Phys. Chem. A* 2021, **125**, 3841-3851.
21. Y. Shao, M. Head-Gordon and A.I. Krylov, The spin-flip approach within time-dependent density functional theory: theory and applications to diradicals. *J. Chem. Phys.* 2003, **118**, 4807-4818.
22. F. Wang and T. Ziegler, Time-dependent density functional theory based on a noncollinear formulation of the exchange-correlation potential. *J. Chem. Phys.* 2004, **121**, 12191-12196.
23. F. Wang and T. Ziegler, The performance of time-dependent density functional theory based on a noncollinear exchange-correlation potential in the calculations of excitation energies. *J. Chem. Phys.* 2005, **122**, 074109.
24. Y.A. Bernard, Y. Shao and A.I. Krylov, General formulation of spin-flip time-dependent density functional theory using non-collinear kernels: theory, implementation, and benchmarks. *J. Chem. Phys.* 2012, **136**, 204103.
25. D. Casanova and A.I. Krylov, Spin-flip methods in quantum chemistry. *Phys. Chem. Chem. Phys.* 2020, **22**, 4326-4342.
26. A.I. Krylov, Spin-flip configuration interaction: an electronic structure model that is both variational and size-consistent. *Chem. Phys. Lett.* 2001, **350**, 522-530.
27. A.I. Krylov, Size-consistent wave functions for bond-breaking: the equation-of-motion spin-flip model. *Chem. Phys. Lett.* 2001, **338**, 375-384.
28. A.I. Krylov and C.D. Sherrill, Perturbative corrections to the equation-of-motion spin-flip self-consistent field model: application to bond-breaking and equilibrium properties of diradicals. *J. Chem. Phys.* 2002, **116**, 3194-3203.
29. L.V. Slipchenko and A.I. Krylov, Singlet-triplet gaps in diradicals by the spin-flip approach: a benchmark study. *J. Chem. Phys.* 2002, **117**, 4694-4708.
30. S.V. Levchenko and A.I. Krylov, Equation-of-motion spin-flip coupled-cluster model with single and double substitutions: theory and application to cyclobutadiene. *J. Chem. Phys.* 2004, **120**, 175-185.

31. A.I. Krylov, Equation-of-motion coupled-cluster methods for open-shell and electronically excited species: the hitchhiker's guide to Fock space, *Annu. Rev. Phys. Chem.* 2008, **59**, 433-462.
32. M.J. Frisch, G.W. Trucks, H.B. Schlegel, G.E. Scuseria, M.A. Robb, J.R. Cheeseman, G. Scalmani, V. Barone, B. Mennucci, G.A. Petersson *et al.* Gaussian 09, Gaussian, Inc.: Wallingford, CT, 2009.
33. E. Epifanovsky, A.T.B. Gilbert, X. Feng, J. Lee, Y. Mao, N. Mardirossian, P. Pokhilko, A.F. White, M.P. Coons, A.L. Dempwolff *et al.* Software for the frontiers of quantum chemistry: An overview of developments in the Q-CHEM 5 package. *J. Chem. Phys.* 2021 (in press).
34. M. de Wergifosse, C. Bannwarth, P. Shushkov and S. Grimme, Stda program for computing excited states and response properties via the simplified TD-DFT methods, version 1.6.2. Code available at <https://github.com/grimme-lab/stda>.
35. N. Baird, Resonance and aromaticity in the lowest $^3\pi-\pi^*$ state of cyclic hydrocarbons. *J. Am. Chem. Soc.* 1972, **94**, 4941-4948.
36. O. El Bakouri, J.R. Smith and H. Ottosson, Strategies for design of potential singlet fission chromophores utilizing a combination of ground-state and excited-state aromaticity rules. *J. Am. Chem. Soc.* 2020, **142**, 5602-5617.
37. G. Oklem, X. Song, L. Toppare, D. Baran and G. Gunbas, A new NIR absorbing DPP-based polymer for thick organic solar cells. *J. Mater. Chem. C* 2018, **6**, 2957-2961.
38. Q. Liang, J. Xu, J. Xue and J. Qiao, Near-infrared-II thermally activated delayed fluorescence organic light-emitting diodes. *Chem. Commun.* 2020, **56**, 8988-8991.